

## STABLE ISOTOPES INVESTIGATION AT HIGH SULPHIDATION GEDABEY GOLD COPPER DEPOSIT (LESSER CAUCASUS)

Sabuhi M. Mammadov<sup>a\*</sup>, Nazim A. İmamverdiyev<sup>b</sup>

<sup>a</sup>*Azerbaijan International Mining Company*

<sup>b</sup>*Baku State University, Baku, Azerbaijan*

DOI: <https://doi.org/10.30546/209805.2025.2.1.145>

---

### Abstract

The article is devoted to the isotope and the temperature estimates derived from sulphide-sulphide and sulphide-sulphate equilibrium calculations at the Gedabey gold copper deposit. Data analysis of the isotopic evidence indicates that mineralisation at Gedabek was driven by a dynamic magmatic-hydrothermal system, with evolving fluid conditions from reduced to more oxidized states, and complex fluid-rock interactions influenced by structural controls.

*Keywords:* Gedabey, stable sulphur isotopes

---

\*Corresponding author.

*E-mail address:* [sabuhi.mammadov@aimc.az](mailto:sabuhi.mammadov@aimc.az) (S. Mammadov)

### Geological features of the area

The primary geological features of the Gedabay deposit are largely determined by its location within the Gedabay-Garadagh volcano-plutonic structure, a major central-type formation characterized by a highly complex internal architecture [1]. The Gedabay ore district is situated on the Shamkir uplift, part of the Lok-Garabagh structural-formational zone of the Lesser Caucasus meganticlinorium. Both the tectonic structure and magmatic history of the Gedabay ore district, as well as the deposit itself, are notably intricate.

During the Middle Jurassic period, the region experienced intense magmatic activity, which can be subdivided into three distinct phases: Bajocian, Bathonian, and Upper Jurassic. The Bajocian phase is further divided into two substages: the Lower Bajocian, which is marked by pyroclastic volcanic rocks and disrupted mafic to intermediate volcanic formations; and the Upper Bajocian, dominated by felsic magmatic rocks [2]. These rock types are widely represented across various facies throughout the Gedabay ore district [3].

Rocks associated with the Bathonian magmatic phase—primarily andesites and, to a lesser extent, andesite-basalt formations—along with pyroclastic materials and lava flows from the Upper Jurassic, are mostly distributed along the flanks of the ore district. Within fracture zones and their surrounding

areas, as well as along microcracks, rocks have undergone significant structural deformation and hydrothermal alteration, resulting in kaolinization, sericitization, and, frequently, the formation of secondary quartzites.

There is limited structural complexity observed within the Lower Bajocian rocks along fault lines. The primary geological overprint is attributed to Upper Bajocian magmatism, particularly along the Gadabay-Bittibulag fault. This phase is characterized by the emplacement of subvolcanic bodies—rhyolites, rhyodacites, and quartz-porphyrries—that began cooling at shallow crustal levels [1]. In the central part of the deposit, tectonic breccia lenses have been identified. Dykes are commonly hosted within andesitic tuffs and porphyritic secondary quartzites (quartz porphyries), all of which have undergone significant hydrothermal transformation. These changes are especially prominent along subvolcanic intrusions and vein-type rock bodies, where multiple styles of alteration are observed.

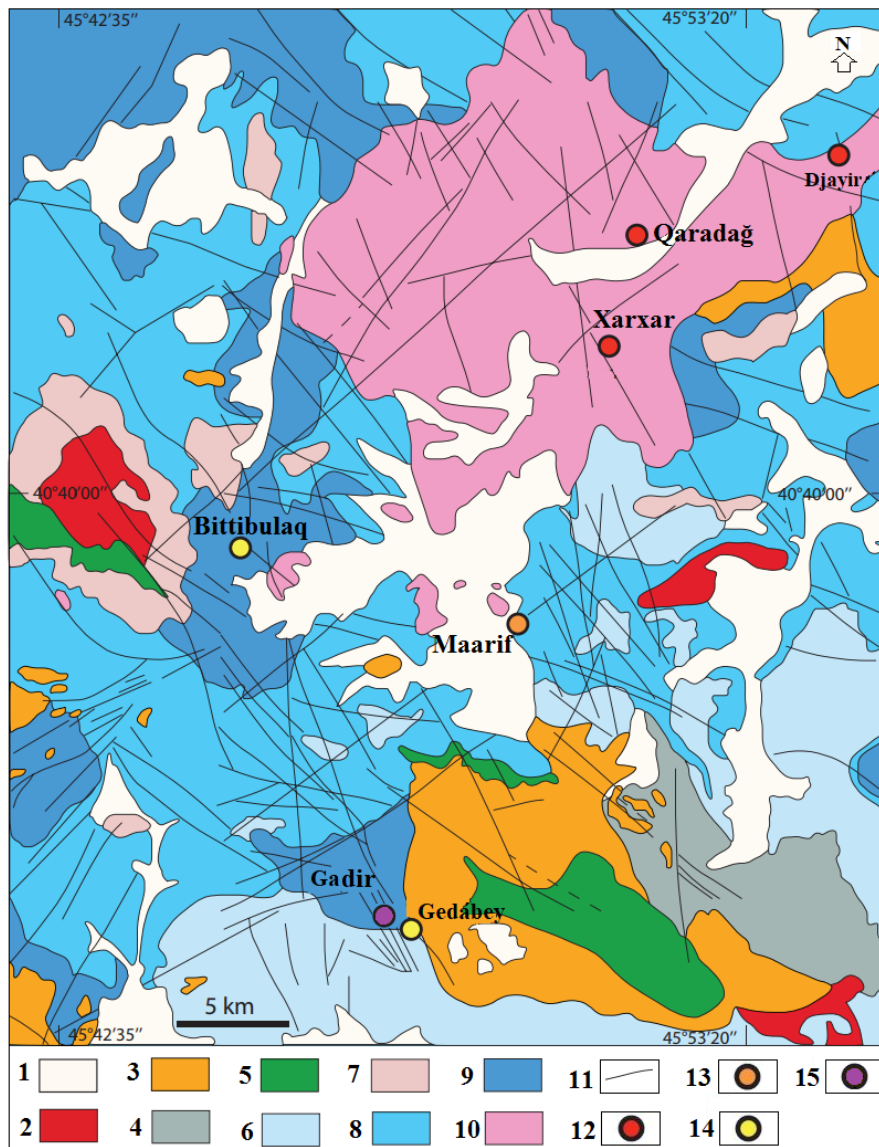


**Fig. 1.** Geological map of the Gedabek district with location of ore occurrences. (Vagif Ramazanov; Pers. Map)

**Legend (Map Symbols):** 1. Quaternary sedimentary deposits; 2. Kimmerian-aged quartz diorite and diorite intrusive rock complex; 3. Kimmerian-aged granodiorite and quartz diorite intrusive rock complex; 4. Callovian–Oxfordian-aged pyroclastic rocks; 5. Gabbroic intrusions (gabbroids); 6. Bathonian-aged volcanogenic and pyroclastic andesitic rock formations; 7. Bajocian-aged subvolcanic rhyolites, dacites, and rhyodacites; 8. Late Bajocian-aged rhyodacites, rhyodacitic tuffs, and tuff breccias; 9. Early Bajocian-aged andesitic porphyries along with associated tuffs and tuff breccias; 10. Early Bajocian-aged plagiogranites; 11. Faults; 12. Porphyry copper-type deposits; 13. Porphyry copper-type occurrences; 14. High-sulfidation epithermal-type deposits; 15. Low-sulfidation epithermal-type deposits

## Investigations of stable isotopes

### Sulphur isotopes

To better understand the temperature conditions, chemical environment, and sulphur source associated with mineralisation at Gedabey, sulphur isotope analyses were conducted on key mineralisation types obtained from the open pit.

A total of 20 samples—comprising 18 sulphides and 2 sulphates—were collected from 13 mineralised zones within the Gedabey open pit and from a drill core. These data are summarized in Table 1 and illustrated in Figure 2. The precision of the results was consistently high, with excellent reproducibility in most cases.

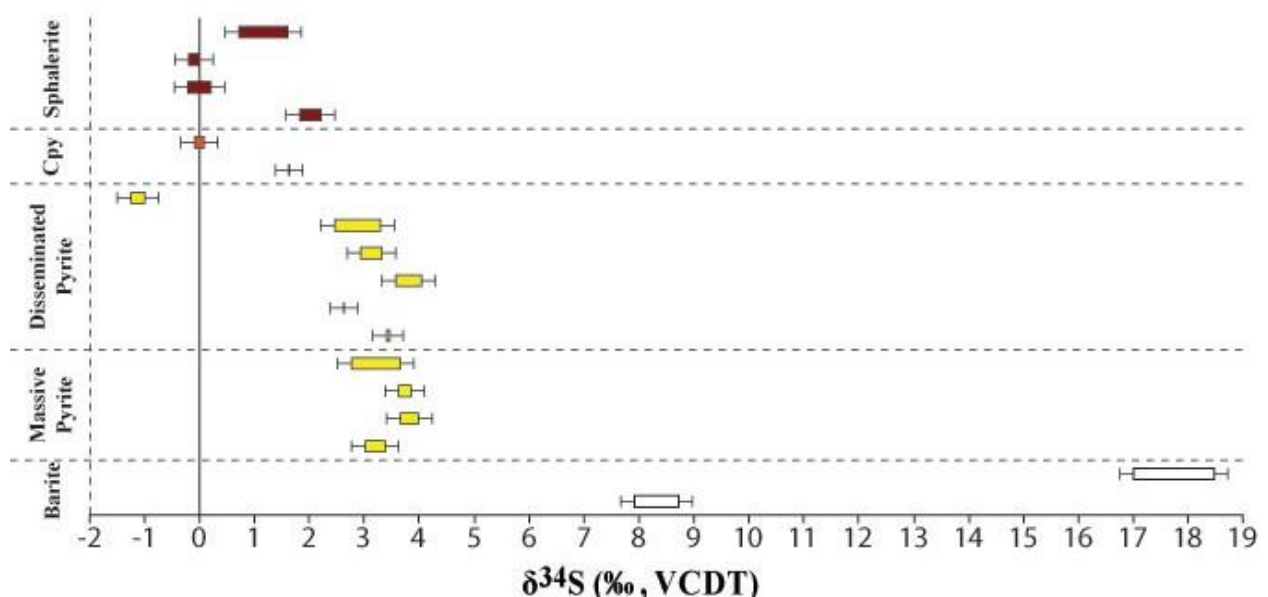


**Fig. 2.** Sulphur isotopes compositions of samples from the Gedabey ore deposit. By University of Lausanne, Switzerland.

This sulphur isotope analyses have been made based on VCDT standard. The term “sulphur isotope related to VCDT” refers to a stable isotope ratio of sulfur, specifically the ratio of sulfur-34 (<sup>34</sup>S) to sulfur-32 (<sup>32</sup>S), measured relative to a standard called VCDT. VCDT stands for Vienna Canyon Diablo Troilite, an international reference standard for sulfur isotope ratios. It’s a lab-prepared standard that replaced the original "Canyon Diablo Troilite" (a sample of meteoritic origin)

The two barite samples yielded notably different isotopic signatures. The heavier barite ( $\delta^{34}\text{S}$  between 7.9‰ and 8.7‰) occurs as large crystals and is spatially associated with pyrite and chalcopyrite, sampled from a drill core approximately 80 meters below surface. In contrast, the lighter barite ( $\delta^{34}\text{S}$  between 17.0‰ and 18.5‰) appears as fine-grained aggregates associated with disseminated fine pyrite and sphalerite, and was sampled at the surface.

Most pyrite samples display  $\delta^{34}\text{S}$  values within a narrow range of 2.5‰ to 4.0‰. These are primarily linked to the quartz-adularia-pyrite mineralisation phase, though two are associated with chalcopyrite and Fe-rich sphalerite from the chalcopyrite-sphalerite phase. One pyrite sample stands out with significantly lower  $\delta^{34}\text{S}$  values (-1.2‰ to -1.0‰) and is in equilibrium with Fe-poor sphalerite from the same mineralisation stage.

The  $\delta^{34}\text{S}$  values for sphalerite and chalcopyrite are also tightly clustered, ranging from -0.2‰ to 2.2‰, aligning closely with the pyrite values. All these samples belong to the chalcopyrite-sphalerite-dominated mineralisation phase.

Table 1.  $\delta^{34}\text{S}$  values of sulphides and sulphates, Gedabek.

Sample no.	Mineral	Mineralisation	Min. style	d34S (VCDT)	duplicate
GE-11-01 A	Barite	Qt-Ad-Py	Disseminated	2,05	3,24
GE-11-01 D	Barite	Isolated	Saccaroide	17,00	18,46
GE-11-02 C	Pyrite	Cp-Sp (Fe-poor)	Disseminated	-1,24	-0,99
GE-11-04 A	Pyrite	Qt-Ad-Py	Disseminated	3,41	3,47
GE-11-04 B	Pyrite	Qt-Ad-Py	Semi-massive	3,03	3,38
GE-11-04 D	Pyrite	Qt-Ad-Py	Semi-massive	3,64	3,84
GE-11-05 A	Chalcopyrite	Cp-Sp (Fe-rich)	Semi-massive	-0,06	0,12
GE-11-05 A	Sphalerite	Cp-Sp (Fe-rich)	Semi-massive	-0,23	0,17
GE-11-05 B	Chalcopyrite	Cp-Sp (Fe-rich)	Large Vein	1,64	1,65
GE-11-05 B	Sphalerite	Cp-Sp (Fe-rich)	Large Vein	1,83	2,21
GE-11-16 B	Pyrite	Qt-Ad-Py	Disseminated	2,64	-
GE-11-26	Pyrite	Qt-Ad-Py	Disseminated	4,03	3,58
GE-11-26	Pyrite	Qt-Ad-Py	Semi-massive	3,66	3,98
GE-11-27	Pyrite	Qt-Ad-Py	Disseminated	2,47	3,29
SGS.DD.99-79,15	Barite	Cp-Sp (Fe-rich)	Large Vein	7,92	8,72
SGS.DD.99-79,15	Sphalerite	Cp-Sp (Fe-rich)	Large Vein	-0,14	0,05
SGS.DD.99-80,50	Pyrite	Cp-Sp (Fe-rich)	Large Vein	2,76	3,65
SGS.DD.99-80,50	Sphalerite	Cp-Sp (Fe-rich)	Large Vein	0,71	1,60

Analytical Error : +/- 0.3‰

### Source of sulphur

The  $\delta^{34}\text{S}$  values of pyrite suggest that both disseminated and semi-massive forms likely originated from the same hydrothermal fluid, including those found in equilibrium with Fe-rich sphalerites from the chalcopyrite-sphalerite-dominated stage. However, the sole pyrite sample associated with Fe-poor sphalerite displays significantly lower  $\delta^{34}\text{S}$  values. Although data for this specific sample are limited, the isotopic composition implies that it may have formed from a different fluid source during this phase of mineralisation.

The presence of pyrrhotite inclusions—observed within both the quartz-adularia-pyrite assemblage and in large chalcopyrite grains in equilibrium with Fe-rich sphalerite—indicates that these mineral phases developed under reducing conditions [4]. As a result, all sulphides analyzed appear to have precipitated in a system dominated by  $\text{H}_2\text{S}$  as the primary sulphur species (see Fig. 3).

In reduced systems, the  $\delta^{34}\text{S}$  values of sulphide minerals closely match the  $\delta^{34}\text{S}$  of  $\text{H}_2\text{S}$  in the fluid—typically within 0.1‰—under conditions of neutral pH and temperatures below approximately 350°C.

Based on this relationship, it can be inferred that:

$$\delta^{34}\text{S}_{\Sigma\text{S}} \approx \delta^{34}\text{S}_{\text{H}_2\text{S}} \approx \delta^{34}\text{S}_{\text{Sulphides}}$$

The average  $\delta^{34}\text{S}$  values of sulphide minerals (Fig. 2) suggest that the  $\delta^{34}\text{S}$  of  $\text{H}_2\text{S}$  in the mineralising fluid was approximately +1‰. This value (−3‰ to +9‰) falls within the typical range for sulphur sourced from igneous systems [5] and supports the interpretation that sulphur was introduced either through direct magmatic fluids or by the leaching of igneous sulphide minerals [6].

### Hydrolysis of $\text{SO}_2$

The hydrolysis of  $\text{SO}_2$  is widely considered a key process in the formation of both sulphide and sulphate minerals in porphyry-copper and epithermal systems [4]. This reaction typically occurs at temperatures below ~350°C, during the cooling of  $\text{SO}_2$ -rich hydrothermal fluids. As the fluid cools,  $\text{SO}_2$  undergoes hydrolysis, producing  $\text{H}_2\text{S}$ —characterized by relatively lighter sulphur isotopes—and  $\text{SO}_4^{2-}$ , which carries heavier sulphur isotopic signatures (see Fig. 4). As temperature continues to decrease, the equilibrium of the hydrolysis reaction progressively favors the formation of  $\text{H}_2\text{S}$  and  $\text{SO}_4$  [6].

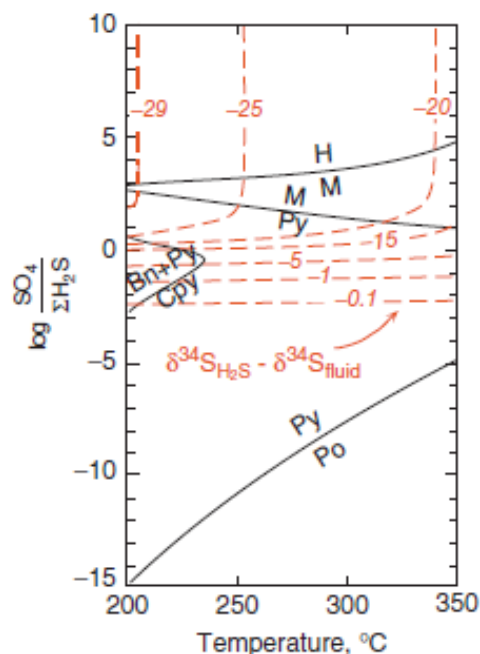
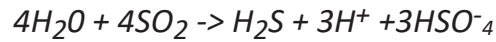


**Fig. 3.** Deviation of  $\delta^{34}\text{S}$   $\text{H}_2\text{S}$  from  $\delta^{34}\text{S}$  fluid as a function of  $T$  and  $\Sigma\text{SO}_2\text{-}24 / \Sigma \text{H}_2\text{S}$  ratio of fluid at pH neutral (Ohmoto and Goldhaber (1997)). Abbreviations: Bn = bornite; Py = pyrite; Cpy = chalcopyrite; Po = pyrrhotite; M = magnetite; H = hematite.



This phenomenon explains the gap of  $\delta^{34}S$  values between sulphides and sulphates (Fig. 2) which is diagnostic for hydrolysis product. Furthermore, the evolution from a smaller fractionation at depth toward a higher fractionation at the surface, with a slightly varying  $\delta^{34}S$  values of sulphides, is typical of an evolution of a “reducing pathway”.

The single pyrite sample in equilibrium with Fe-poor sphalerite shows a  $\delta^{34}S$  value that is shifted toward negative values. While the data available is insufficient to definitively confirm this interpretation, the result is consistent with the higher barite content observed and the transition to more oxidized fluid conditions.

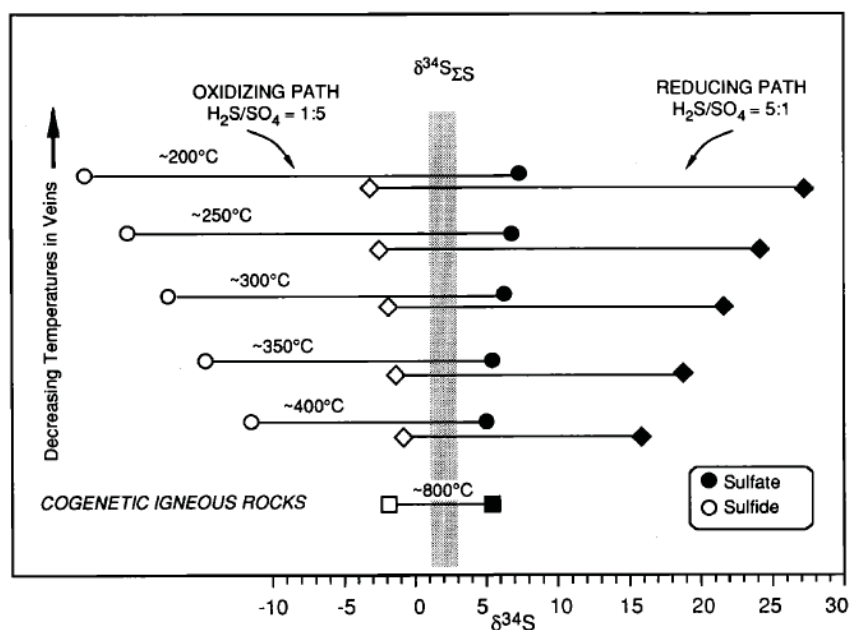


**Fig. 4.** Idealized  $\delta^{34}S$  systematic of coexisting sulphides and sulphates derived from evolved magmatic fluid with initial  $H_2S/SO_2=1$  and precipitated over the temperature range  $400^\circ$  to  $200^\circ C$  [7]

#### Temperature estimate

Sulphide minerals that formed in equilibrium from the same fluid and are spatially associated were used to estimate the temperature conditions during mineralisation [4]. The calculations and the results are shown in Figure 5. All temperature estimates are related to the chalcopyrite-sphalerite-dominated stage of mineralisation. The geothermometer based on the equilibrium between chalcopyrite and sphalerite suggests temperatures ranging from 227 to 952°C. The pyrite-sphalerite equilibrium gives a temperature range between 48 and 96°C, while the temperature estimate using barite and sphalerite from depth (~80m) suggests values between 610 and 660°C.

The barite-sphalerite and chalcopyrite-sphalerite pairs yield unusually high temperature estimates (~660°C and ~952°C, respectively), while the pyrite-sphalerite pair suggests an unrealistically low temperature. These highly variable temperature estimates can be explained by disequilibrium, where the observed isotopic fractionation ( $\Delta_{\text{observed}}$ ) is generally smaller than the equilibrium fractionation ( $\Delta_{\text{equilibrium}}$ ). At temperatures below ~300°C, isotopic equilibrium between coexisting sulphides and sulphates is not always achieved [6]. Disequilibrium between mineral pairs is often attributed to fluctuations in the  $\text{SO}_4/\text{H}_2\text{S}$  ratio of the fluid, as well as short residence times (less than one month) that prevent full isotopic equilibrium. Consequently, the rapid cooling of the fluid, which disrupts sulphur isotope equilibrium, can account for the unrealistic temperature estimates derived from sulphide-sulphate pairs. Another potential cause of fluid disequilibrium is fluid mixing, leading to variations in the  $\text{SO}_4/\text{H}_2\text{S}$  ratio [8]

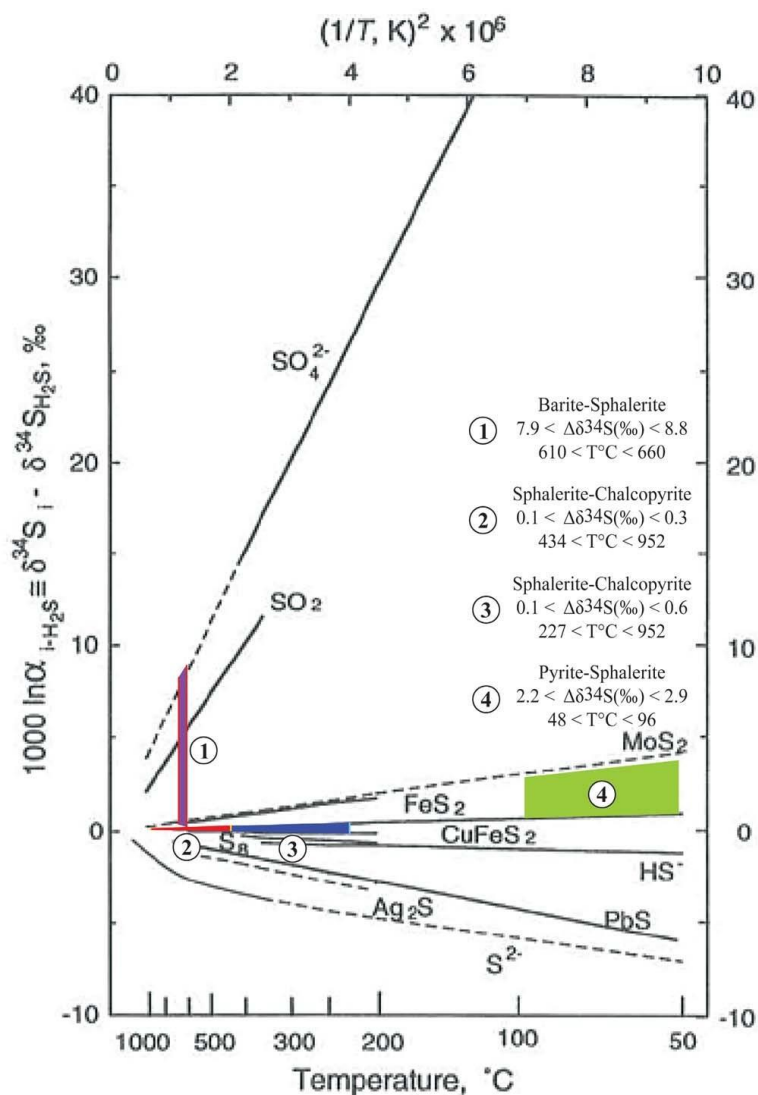


**Fig. 5.** Temperature estimates of sulphide-sulphide and sulphide-sulphate pairs, based on the isotopic fractionation factors between sulphur compounds (i) and  $\text{H}_2\text{S}$ . Solid lines: experimentally determined; dashed lines: extrapolated or theoretically calculated.

## Conclusion

Isotopic analyses of sulphur at the Gedabey deposit provide valuable insights into the nature and evolution of the mineralising system. Sulphur isotope data ( $\delta^{34}\text{S}$ ) suggest that most sulphide minerals formed from a reduced, magmatic-derived hydrothermal fluid where  $\text{H}_2\text{S}$  was the dominant sulphur species. The close  $\delta^{34}\text{S}$  values of pyrite, chalcopyrite, and sphalerite, along with the positive  $\delta^{34}\text{S}$  signature ( $\sim +1\%$ ), support an igneous source of sulphur, either from magmatic fluids or the leaching of igneous sulphides.

The significant isotopic fractionation observed between sulphides and sulphates is characteristic of  $\text{SO}_2$  hydrolysis during cooling, producing isotopically light  $\text{H}_2\text{S}$  and heavy  $\text{SO}_4$ . The increasing sulphur isotope fractionation toward the surface, along with petrological evidence, reflects a transition from deep, reduced conditions to more oxidized, near-surface environments — consistent with a "reducing pathway" evolution.

Temperature estimates derived from sulphide-sulphide and sulphide-sulphate equilibrium calculations are highly variable and, in some cases, unrealistic. This inconsistency likely reflects disequilibrium caused by rapid fluid cooling, short fluid residence times, or fluid mixing events that altered the  $\text{SO}_4/\text{H}_2\text{S}$  ratio, preventing full isotopic equilibration.

Overall, the isotopic evidence indicates that mineralisation at Gedabek was driven by a dynamic magmatic-hydrothermal system, with evolving fluid conditions from reduced to more oxidized states, and complex fluid-rock interactions influenced by structural controls.

## References

1. Babazadə V.M. (2013). *Geology of Mineral Deposits. Part II: Textbook* (in Azerbaijani). Baku: 498 pages.
2. Dilek Y, İmamverdiyev N, Altunkaynak Å (2009) Geochemistry and tectonics of Cenozoic volcanism in the Lesser Caucasus (Azerbaijan) and the peri-Arabian region: collision-induced mantle dynamics and its magmatic fingerprint. *International Geology Review* 52: 536-578.
3. İmamverdiyev N., Orudzhov A., Valiyev A. et al. (2022). Petro-geochemical features of the Bajocian island-arc volcanism in the Lesser Caucasus (Azerbaijan). *Journal of Geology, Geography and Geoecology*, Kyiv: V.31 (2), p. 280-292.
4. Hemon, Pierre The Gedabek quartz-adularia-pyrite altered, Cu-Au-Ag epithermal deposit, Western Azerbaijan; Lesser-Caucasus: Geology, alteration, mineralization, fluid evolution and genetic model: MScThesis / Geneva, 2013, - 87 p
5. Ohmoto H, Goldhaber (1997) Sulfur and carbon isotopes. *Geochemistry of hydrothermal ore deposits* 3: 517-600.
6. Ohmoto H, Rye R (1979) Isotopes of sulfur and carbon. *Geochemistry of hydrothermal ore deposits*: 509-567.
7. Rye RO (1993) The evolution of magmatic fluids in the epithermal environment; the stable isotope perspective. *Economic Geology* 88: 733-752.
8. Zheng YF (1991) Sulfur isotopic fractionation between sulfate and sulfide in hydrothermal ore deposits: disequilibrium vs equilibrium processes. *Terra Nova*, 3, 510-516. (Zheng, 1991).